

FRACTURE ENERGY OF SELECTED BRITTLE SILICATES

[#]PETR JANDAČKA, JINDŘICH ŠANCER*, HANA VOJTKOVÁ**, PETR BESTA***,
ROBERT BRÁZDA****, PETRA KOLIČOVÁ**, LUCIE ŠIMKOVÁ**

*Nanotechnology Centre and Institute of Physics, VŠB-Technical University of Ostrava
17. listopadu 15, 70833 Ostrava, Czech Republic*

** ICT, VŠB-Technical University of Ostrava*

***Institute of Environmental Engineering, VŠB-Technical University of Ostrava*

****Department of Economics and Management in Metallurgy, VŠB-Technical University of Ostrava*

***** Institute of Transport, Technical University of Ostrava*

[#]E-mail: petr.jandacka@vsb.cz

Submitted May 13, 2011; accepted September 26, 2011

Keywords: Fracture energy, Surface energy, Specific surface, Powder

In this research, the specific fracture energy of almandine, zircon and periclase (MgO) are presented. The materials measured were in powder form during the measurement. A method of crushing the materials using a hydraulic press was used, followed by statistical analysis of the change in the surface of the powder. Values were taken from particle size measurements performed by a laser analyzer for the specific surface area calculation. Additionally, the surface energy was calculated for periclase based on these measured values in order to evaluate whether the measurement was valid in comparison to the measured values specified by other authors. The dependency of specific fracture energy on crushing speed and environment in which the powder was crushed (air or water) was also analyzed.

INTRODUCTION

One of the important parameters used to characterize surface phenomena in solid substances is the specific surface energy. For fracture processes, it is then a special case of specific surface energy, namely the specific fracture energy [1-5]. However, there is very little information available concerning the values of specific fracture energy in the literature. Most contributions from the area of fracture mechanics deal with various fracture criteria and only a few of these contributions deal with the general measurements of specific fracture energy, apparently due to the difficulty in measuring this quantity. The publication [6, p362] shows the following: Austin's comment on the experiment of measurement of surface energy based on the energy balance of grinding process." Experiments on mills show that the fraction of the electric power input to the mill, which is used directly to break bonding forces, is very small (smaller than one percent) and is usually less than the error involved in the measurement of the energy balance."

A frequently cited work in the case of specific surface energy measurements of brittle materials is that of Gilman [7], who used the monocrystal cleavage method to break the material along a prepared crack. His work shows the specific surface energy (cleavage

energy) for various crystallographic planes of LiF, MgO, CaF₂, BaF₂, CaCO₃, Si, Zn, and Fe (3% Si) monocrystals at various temperatures and in various environments. In their report, Davidge and Tappin [8] used a three-point bending test with the subsequent crystal fracture. Additionally, these authors differentiate between the specific surface energy in the fracture initiation and its effective value over the entire fracture process. The same method was used by Nakayama, Friedman et al., and Messmer and Bilello [1, 2, 9]. They determined the surface energy of Si, GaAs, and GaP using Griffith's criterion for brittle fracture [10, 11] specifically on the basis of critical stress in a sample from the length of a crack. Smith et al. [3] used a similar method but they made a detailed analysis of the new surface irregularities through the use of fractal geometry parameters. Specific fracture energy and fracture toughness values for a total of 48 minerals were calculated theoretically based on available data by Tromans and Meech [12]. Their calculations were based on Born's interactive model of matter structural particles (ions).

The goal of this article is to present the results of specific fracture energy measurements of almandine, zircon, and periclase. Additionally, the surface energy has been determined for periclase in order to evaluate the measurement's validity. The influence of crushing

speed and environment (air or water) on specific fracture energy values has also been investigated. In addition to their general applicability, the measurements of mineral fracture energy made in this study, shown below, can be used in the study of abrasive and milling properties [13-16]. The method of crushing the minerals into powder form using a hydraulic press, presented previously in Jandačka et al. [17], was used.

MATERIALS AND METHOD

This work measured three minerals whose basic characteristics are shown in Table 1.

Specific fracture energy was determined using the initial fragmentation of the powders by crushing and computing the change in surface area. The statistical parameters of the powders were measured using a laser analyzer Mastersizer 2000 type 5.4 (Malvern Instruments Ltd). The main device for measurement was a steel-corundum crusher of the author's own design (Figure 1).

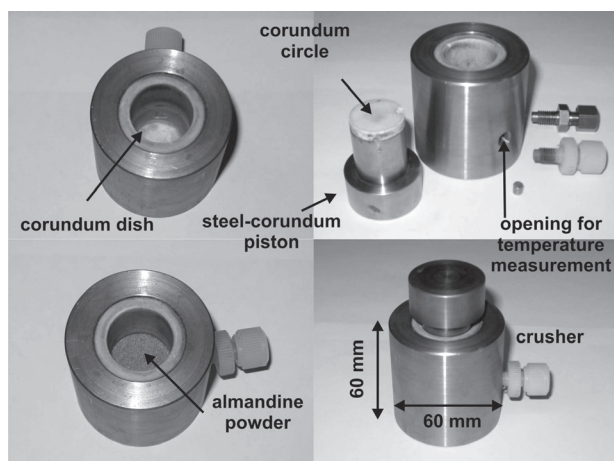


Figure 1. The crusher.

The force on the piston was realized using a very precise hydraulic press MTS 816 Rocks Test System (MTS System Corporation). Special software recorded the applied force and displacement. A more detailed description of this method is described in Jandačka et al. [17].

During the above-mentioned crushing, there were two phases, which are shown by the curves in Figure 2. The first phase was a compression phase, in which the compression work W_{com} is expressed by the compression force F_{com} (Equation 1a). The second phase was the compression unloading phase, expressed by the unloading force F_{up} .

The compression unloading work W_{up} (Equation 1b) represents the potential energy of elasticity of the compressed system (powder and crusher) and, at the same time, the energy which is returned to the press. The crushing work W_{cru} needed to change the powder surface is defined in Equation 2.

$$W_{com} = \int_0^{x_1} F_{com} dx, \quad W_{up} = - \int_{x_1}^{x_2} F_{up} dx, \quad (1a, 1b)$$

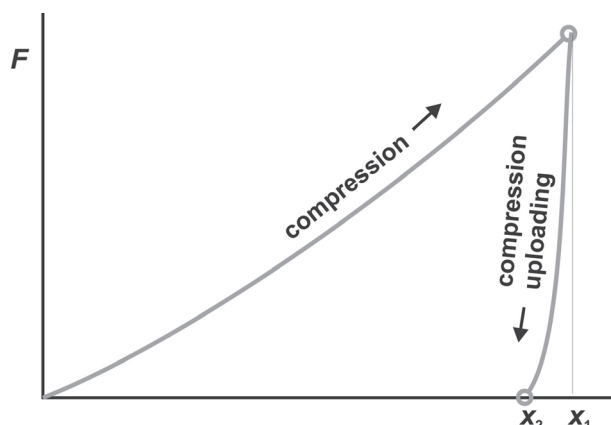


Figure 2. General schematic of compression of powder by a hydraulic press.

Table 1. Basic characteristics of the measured powders.

Characteristics	Almandine	Zircon	Magnesium oxide (periclase)
chemical formula	$Fe_3Al_2Si_3O_{12}$	$ZrSiO_4$	MgO
mineralogical purity	97	94-98	98
commercial name	Australian garnet	Zircon sand	Magnesium oxide
origin	Australia	RSA	-
manner of preparation	mining, processing	mining, processing	synthesis, crushing
original particle size (μm)	100-200	100-200	< 500
particle density (kg/m^3)	4084	4617	3580
observed particle shape	irregular	irregular	irregular
particle approximation by*	sphere	sphere	sphere
cleavage	none	imperfect {110}	perfect {100}
crystallographic system	cubic	tetragonal	cubic
Mohs' hardness	7.5	8	5.5
spec. heat capacity ($J/kg \cdot K$)	-	-	922

* These powders consisted primarily of monocrystalline particles

$$W_{\text{cru}} = W_{\text{com}} - W_{\text{up}} \quad (2)$$

Theoretical smoothing of the measured points was performed using an n -th grade polynomial. Reliability of all performed smoothing was higher than 0.98, i.e., $R^2 > 0.98$.

Krycer et al. [18] stated that the different force effects of a press on the top and bottom of the base of a die must be taken into account. This difference is caused by the friction of particles along the die wall. This phenomenon is considered negligible in this study. The reason for this simplification is that in the crusher used, particle-die wall abrasion is restricted by the corundum die wall, i.e., the die wall was harder than the powder particles. In general, the mechanical work of the press is transferred to seven types of energy: surface energy, surface plastic deformation, interparticle friction, the above-mentioned particle-corundum friction, van der Waals forces between particles, the energy of powder compaction (restriction of particle flow), and the potential energy of elasticity of the compressed system (powder and crusher) [18-24]. In this study, we will consider only the first three energy phenomena. Because we are using very brittle minerals and a corundum die, this focus on just three energy phenomena is valid.

The act of crushing a mineral changes the powder temperature. In these experiments, several methods for measuring powder temperature (for example, using the side opening on the crusher, see Figure 1a) were tried but in the end the most precise method was by using a "surface thermocouple sensor". This sensor was placed on top of the powder from above, both before and after crushing.

Theoretical background

The next subchapter presents application equations related to the author of this contribution, previously and similarly presented in [17]. They are based on a fundamental knowledge of fracture mechanics [10, 11, 25-28] and the basic laws of thermodynamics. The specific fracture energy can be determined using the general equation

$$\text{specific fracture energy} = \frac{\text{work of fracture}}{\text{surface change}} \quad (\text{J/m}^2)$$

Work of crushing

By application of the first law of thermodynamics, assuming that there is no heat exchange between the system and its surroundings (adiabatic phenomenon), the following expressions for mechanical work W_{mech} on a powder in a clear liquid can be obtained:

$$\begin{aligned} \Delta W_{\text{mech}} &= \Delta U = \Delta W_V + \Delta W_A, \\ \Delta W_A &= \gamma_{\text{el}} \Delta a + \gamma_{\text{pl}} \Delta a + \mu \Delta n, \end{aligned} \quad (3)$$

where U is the internal powder energy, W_V is the volume work, W_A is the surface work, γ_{el} is the surface energy related to the vacuum (environment), γ_{pl} is the specific energy of the plastic surface deformation, a is the surface area, μ is the chemical potential, and n is the number of liquid molecules adsorbed at the front of the crack during crushing. The right side of Equation 3 could contain the translational and rotational kinetic energy of the broken particles; however, in this study the term is equal to zero. The surface plastic work $\gamma_{\text{pl}} \Delta a$ is connected to the plastic deformation of the surface layer, in agreement with generally known findings that the fracture of a brittle material is accompanied by a minute area of plastic deformation which surrounds the propagating fracture front [25-28]. Since in the case of brittle substances it can be assumed that plastic deformation occurs only along the front of the propagating crack, the volume term contained in the overall volume plastic deformation term can be excluded. The volume elastic work (a component of W_V) in the case of the above-mentioned measurements is returned to the press during compression uploading. The value $\mu \Delta n$ specifies the interfacial energy and characterizes the environment surrounding the fractured matter. During a slowly propagating fracture, are in the surface area adsorbed maximal amount $n = a/s$ of molecules of liquid, where s is the cross-section of the liquid molecule. However, during a very fast-moving fracture, not all molecules are able to adsorb (diffuse) on the tip of the crack [28-32].

Specific fracture energy and specific surface energy

Equation 2 defines the crushing work W_{cru} . The specific fracture energy can then be calculated according to the expression

$$\sigma_{\text{fra}} = \frac{\Delta W_A}{\Delta a} = \frac{\Delta W_{\text{cru}}}{m \cdot \Delta A_{\text{geo}}} \quad (4)$$

where m is the weight of the powder and ΔA_{geo} is the difference in the specific geometric surface area before and after crushing. The surface energy is then given by the expression

$$\gamma = \frac{\Delta(W_A - \gamma_{\text{pl}} a)}{\Delta a} = \frac{\Delta W_{\text{cru}} - mc \Delta T}{m \cdot \Delta A_{\text{geo}}} \quad (5)$$

where c is the specific heat capacity of the powder and ΔT is the powder temperature change during crushing. The surface energy is given by the larger potential energy of atoms in the surface layer than in the volume. They are pushed out of their regular positions, both in normal and tangential positions [32, p83]. The surface energy is not affected by the mode or speed of crushing. The powder temperature change is connected to the plastic deformation of the powder particles, which in the case of brittle materials lie primarily in the surface layer. The

range of this plastic deformation is influenced by the crushing rate, i.e., plastic deformation cannot propagate with the same velocity as an elastic deformation (crack propagation). During a slowly propagating fracture, significant plastic deformation can be assumed, whereas during a very fast-moving fracture there will be only minimal plastic deformation.

Specific surface area determination

Distribution of powder particles that are prepared by grinding or crushing are usually governed by a logarithmic-normal distribution, i.e., by normal distribution of the $\ln d_i$ values, where d_i are the diameters of the particles, which is the method presented in [33-36]. In this study, the specific surface area is calculated by approximating the particle shape as a smooth sphere. The use of fractal theory for determining the specific area of powders is shown in Jandačka et al. [37]. The specific geometric surface area for a smooth sphere with a log-normal particle size distribution is given as [17, 35, 37]

$$A_{\text{geo}} = \frac{6}{\rho \cdot \exp(\mu + 2.5\omega^2)}, \quad (6)$$

where ρ is the powder particle density (weight of particle/volume of particle). The arithmetic mean μ and selective standard deviation ω can be calculated from the equations [17, 33-36]

$$\mu = \ln d_{0.5} \text{ and } \omega = \frac{1}{1.29} \ln \left(\frac{d_{0.9}}{d_{0.5}} \right). \quad (7a, 7b)$$

Fractiles $d_{0.5}$ and $d_{0.9}$ were determined using laser analyzer software and 1.29 is the tabulated value for $d_{0.9}$ by normal (Gaussian) distribution. Instead of the Equation 6, the expression $A_{\text{geo}} = 6/\rho d$ is often used [37-40], where d is the arithmetic mean.

The specific surface area of the original powder (uncrushed) has negligible size in comparison with the specific surface area of the crushed powder. It is 0.0098 m²/g for almandine, 0.0087 m²/g for zircon, and 0.0034 m²/g for periclase. These three values were calculated according to the special case of Equation 6 in which $\omega = 0$ and $A_{\text{geo}} = 6/\rho d$ (as mentioned above). Since the original (uncrushed) almandine and zircon powders were sieve-differentiated to narrow fractions, the value of ω is negligible.

RESULTS AND DISCUSSION

In total, 37 sample crushings of periclase, almandine, and zircon powders were performed during the experiment. For almandine and zircon there were four compressions using the same regime and in the same environment (water or air) for compression rate increases of 11.8 MPa/s (6 kN/s, crushing time 10 s), and 118 MPa/s (60 kN/s, crushing time 1 s). The final compression of

the press was 118 MPa (60 kN). For MgO, it was five crushings by 5.92 MPa/s (3 kN/s, crushing time 10 s), and the final compression was 59.2 MPa (30 kN). The compression uploading period was set to 0.5 s for all samples. The crusher piston moved the most with the MgO samples, approximately 10 mm. During the crushing, a computer recorded the compression force value F of the press and the movement of the press x with 100 points-per-second frequency. For example, in the almandine sample identified as *aml_5*, which was crushed by 11.8 MPa/s in water, $m = 24.50$ g, $W_{\text{com}} = 113.36$ J, $W_{\text{up}} = 3.50$ J, $x_1 = 4.77$ mm, $x_2 = 4.53$ mm, after crushing: $d_{0.5} = 0.231$ μm , $d_{0.9} = 0.605$ mm, $\Delta A_{\text{geo}} = 1.57$ m²/g, $\sigma_{\text{fra}} = 2.86$ J/m². Particle sizes of powders before and after crushing are shown in Table 2.

Table 2. Particle size change after crushing

Mineral	Initial particle size (μm)	After crushing (average)	
		median $d_{0.5}$ (μm)	the finest particles (μm)
almandine	100-200	0.23	0.20
zircon	100-200	0.38	0.30
periclase (MgO)	500-1000	0.24	0.20

The row data values of the $d_{0.9}$ fractile generally correlate with values of dp/dt , where p is the press on the powder. This evokes an investigation of the dependency of the crushing speed dp/dt on the value of $d_{0.9}$. These dependencies have been thoroughly investigated in Grady's works [41, 42].

Determination of specific fracture energy

The fracture energy values were determined by applying Equation 4 and the surface energy of MgO was calculated according to Equation 5. Figures 3, 4, and 5 show the averaged values of the specific fracture energy of repeated measurements in individual regimes. Standard deviations of the mean of the repeated measurements are marked around the arithmetic mean values, means their highest values for all regimes. The zircon mean standard deviation is overall the highest for all three dispersion matters, namely 13%. From the point of view of the mean standard deviation, it is possible to characterize the measurement as being accurate overall. For example, Gilman's [7] measurements of MgO, during which cleavage of monocrystals was used, Gilman achieved a standard deviation of the mean of 15% for three repeated measurements. By using a very precise hydraulic press and laser analyzer it can be stated that the main source of measurement errors arise from random errors connected to the crushing process. For this reason, it can now be estimated that the total measurement error (uncertainty) does not exceed 15% using this method.

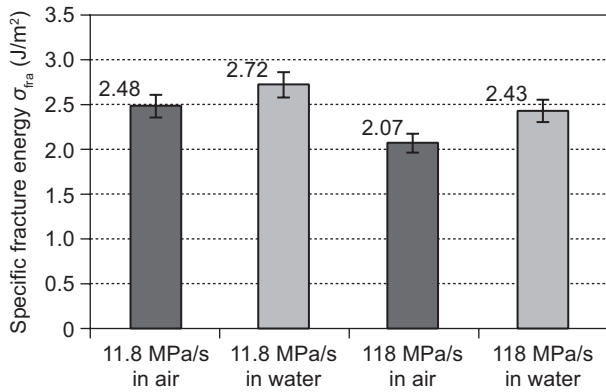


Figure 3. Average values of the specific fracture energy of almandine in applied regimes and their standard deviations of the mean, 5.2%.

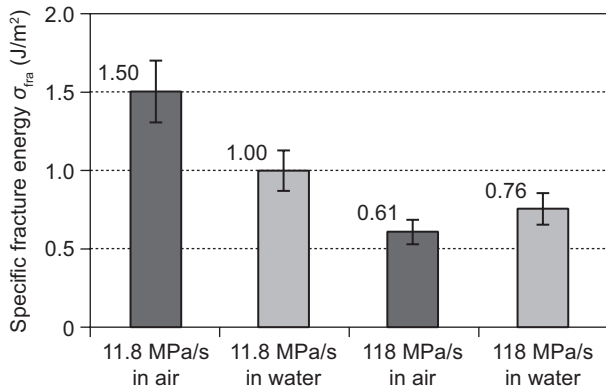


Figure 4. Average values of the specific fracture energy of zircon in applied regimes and their standard deviations of the mean, 13 %.

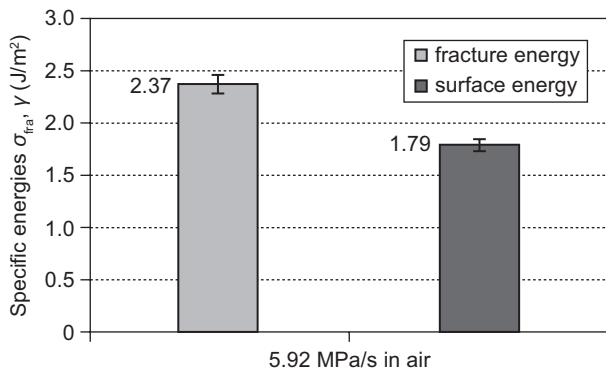
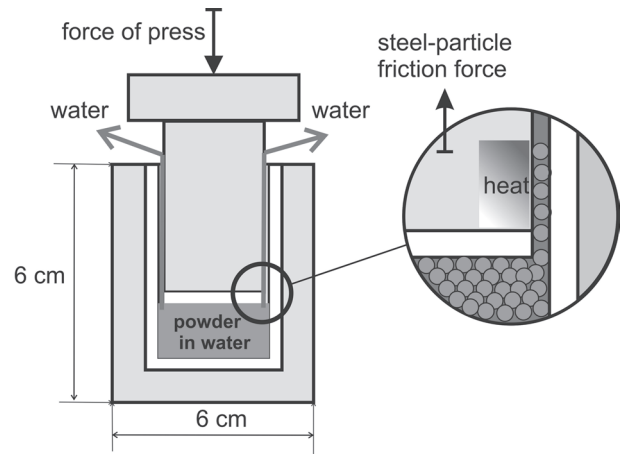


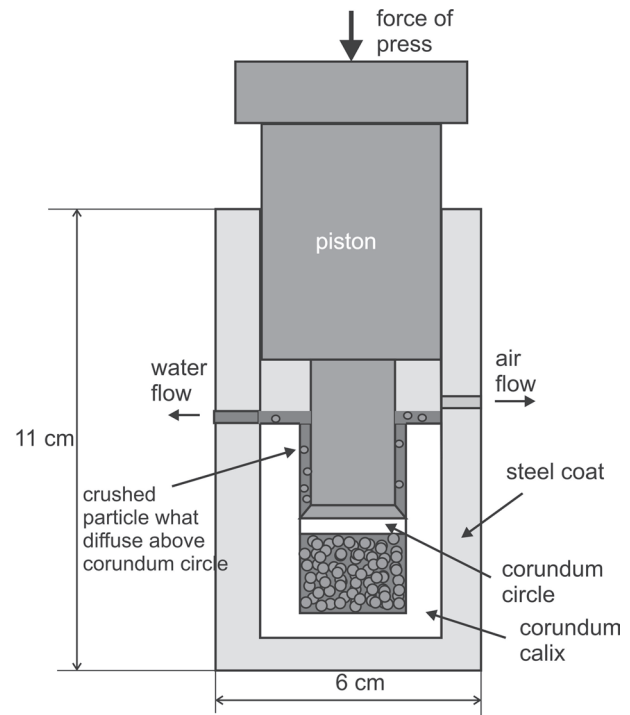
Figure 5. Average values of the specific fracture energy and surface energy of periclase (MgO) in applied regimes and their standard deviations of the mean, 3.8 % and 3.4 %. Surface energy is 76 % of the specific fracture energy.

These graphic results show that the specific fracture energy decreases while the speed of compression increases. This is in agreement with our knowledge of the behavior of dislocations that do not have as much time to shift during faster crushing as when the crushing is slower [43].

More complicated is the dependency of the specific fracture energy on the type of liquid environment in which the fractures take place. This is the meaning of the term $\mu\Delta n$ in Equation 3. In Jandacka et al. [17], there was a decrease of the specific fracture energy observed in the case of crushing in water in comparison with that observed with crushing in air (using a lower final force of press), which is in agreement with Equation 3. This trend, however, is opposite from Figures 3 and 4. This paradox can be explained by the shielding friction that occurs as a result of powder particle abrasion on the piston steel



a)



b)

Figure 6. Schematic of the piston–particles friction during crushing in water (a) and author’s own crusher design which should restrict the shield phenomenon (b).

part above the corundum ring. Figure 6a graphically shows this negative phenomenon and Figure 6b is the author's own design of crusher that should restrict this negative phenomenon.

Changes of powder temperature were also measured in the case of MgO in order to express the surface energy according to Equation 5. For the five above-mentioned measurements (one of them failed), the average temperature change is 1.88 K. The surface energy value serves as an evaluation of the measurement validity within this work, which is 76% of the specific fracture energy.

Validity of measurement

Evaluation regarding whether these measurements were correctly performed is based on the comparison of the MgO surface energy obtained by other authors with the value obtained in this work (Figure 7). The surface energy quantity has been used because it is independent of both the crushing speed and the plastic deformation of surface layers during fracturing.

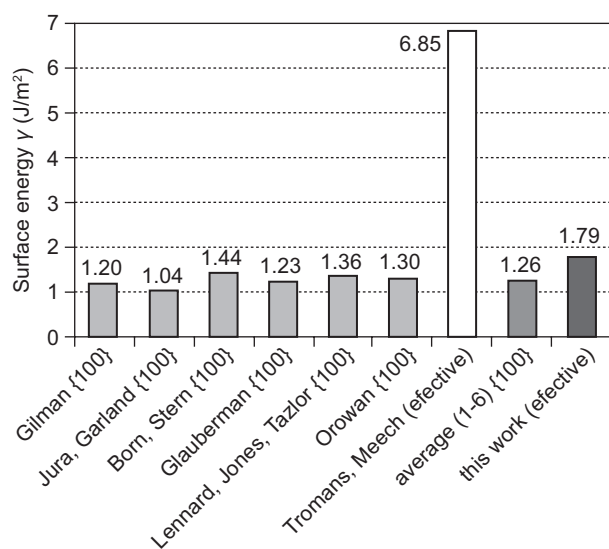


Figure 7. Comparison of surface energy of periclase (MgO) measured by other authors (by theoretical or experimental methods) and in this work. The first six values were transferred from Gilman (1960).

The average value of the MgO surface energy by other authors is 1.26 J/m². This value does not account for Tromans and Meech's [12] outlying value. The value determined within this work is higher, namely 1.79 J/m². All authors with the exception of Tromans and Meech investigated the surface energy along the {100} crystallographic planes. According to Born and Stern [7], however, the MgO surface energy in the {110} planes is 2.7 times larger than it is in the {100} planes. It can be supposed that many cracks go through weakly

bounded planes (by crushing powders). This is one possible explanation why the value of the surface energy measured in this work on randomly oriented particles is higher by 30% compared to the average value of this quantity measured by other authors. From this we can estimate that the measurement was valid and that the approximation of particle shape as smooth spheres did not introduce a significant error into our calculations. However, the measurements of specific fracture energy during crushing in water were probably invalid, as explained above.

CONCLUSION

Specific fracture energy depends on crushing speed. In an air environment and a crushing speed of 11.8 MPa/s, the specific fracture energy was 2.48 J/m² for almandine and 1.50 J/m² for zircon. In an air environment and a crushing speed of 118 MPa/s, the specific fracture energy was 2.07 J/m² for almandine and 0.61 J/m² for zircon. Determination of the specific fracture energies in a water environment were not deemed valid. Explanation of this lies in the above-mentioned shielding phenomenon. This effect can be theoretically restricted using a new crusher design with a cone piston tip (Figure 6b). Base on analysis of the crushing process, the accuracy of the device used was estimated to have a measurement error (uncertainty) of 15%. Using the method of crushing the powder by hydraulic press and subsequent measurement of particle sizes by laser analyzer and approximating the particle shape as a smooth sphere is, for this type of brittle material, valid. This conclusion results from a comparison of our determination of the surface energy of MgO with that of other authors.

Acknowledgements

The authors thank the HGF of the VŠB-Technical University of Ostrava for their support through project name SGS 2011 no. SP2011/123, project IT4 Innovations Centre of Excellence project no. CZ.1.05/1.1.00/02.0070 and unknown reviewer for his critical comments.

References

1. Nakayama J.: J. Amer. Ceram. Soc. 48, 583 (1965).
2. Friedman M., Handin J., Alani G.: Int. J. Rock Mech. Min. Sci. 9, 757 (1972).
3. Smith R.L. III, Mecholsky J.J. Jr., Freiman S.W.: Int. J. Fract. 156, 97 (2009).
4. Park S., Dillard D.A.: Int. J. Fract. 148, 261 (2008).
5. Man H.K., Mier van J.G.M.: Int. J. Fract. 154, 61 (2008).
6. Kaye B.H.: *A Random Walk Through Fractal Dimension*. VCH, New York 1994.
7. Gilman J.J.: J. Appl. Phys. 31, 2208 (1960).

8. Davidge R.W., Tappin G.: *3*, 65 (1968).
9. Messmer C., Bilello J.C.: *J. Appl. Phys.* *52*, 4623 (1981).
10. Griffith A.A.: *Transaction of the Royal Society of London A* *221*, 163 (1920).
11. Anderson T.L.: *Fracture mechanics: fundamentals and applications*. Taylor & Francis, Boca Raton 2005.
12. Tromans D., Meech J.A.: *Minerals Engineering* *15*, 1027 (2002).
13. Urakaev F. Kh.: *Int. J. Miner. Process.* *92*, 58 (2009).
14. Hlavac L.M.: *Journal of Materials Processing Technology* *209*, 4154 (2009).
15. Hlavac L.M., Hlavacova I., Jandacka P., Zegzulka J., Viliamsova J., Vasek J., Mádr V.: *International Journal of Mineral Processing* *95*, 25 (2010).
16. Guo Ch., Dong L.: *Journal of China University of Mining & Technology* *17*, 251 (2007).
17. Jandacka P., Hlavac L.M., Madr V., Sancer J., Stanek F.: *Int J. Fract.* *159*, 103 (2009).
18. Krycer I., Pope D.G., Hersey J.A.: *Drug development and industrial pharmacy* *8*, 307 (1982).
19. Eriksson M., Alderborn G.: *Pharmaceutical Research* *12*, 1031 (1995).
20. Bergh v. d. W.J.B., Scarlett B.: *Powder Technology* *67*, 237 (1991).
21. Kadiri M.S., Michrafy A., Dodds J.A.: *Powder Technology* *157*, 176 (2005).
22. Miller O., Freund L.B., Needleman A.: *Int. J. Frac.* *96*, 101 (1999).
23. Pitchumani R., Zhupanska O., Meesters G.M.H., Scarlett B.: *Powder Technology* *143-144*, 56 (2004).
24. Pugno N.M., Carpinteri A.: *Int. J. Fract.* *149*, 113 (2008).
25. Irwing G.R.: *J. Appl. Mech.* *24*, 361 (1957).
26. Orowan E.: *Weld. J. Res. Suppl.* *34*, 157 (1955).
27. Rice J.R.: *J. Appl. Mech.* *35*, 379 (1968).
28. Adamson W.A.: *Physical Chemistry of Surfaces*. John Wiley & Sons, Inc, New York 1990.
29. Parks G.A.: *Journal of Geophysical Research* *89*, 3997 (1984).
30. Ciccotti M.: *J. Phys. D: Appl Phys* *42*, 18 (2009) (Preprint).
32. Lüth H.: *Solid Surfaces, Interfaces and Thin Films*. Springer, New York 2001.
33. Brantley S.L., Mellott N.P.: *American Mineralogist* *85*, 1767 (2000).
34. Zisselmar R., Kellerwessel H.: *Part. Character.* *2*, 49 (1985).
35. Likes J., Machek J.: *Computation of probability*. SNTL, Prague 1987 (in Czech).
36. Allen T.: *Powder Sampling and Particle Size Determination*. Elsevier, Amsterdam 2003.
37. Jandacka P., Studentova S., Hlavac L.M., Kvicala M., Madr V., Hredzak S.: *Chemické listy* *105*, 146 (2011).
38. Papelis Ch., Um W., Russell Ch.E., Chapman J.B.: *Colloids and Surfaces A: Physicochem. Eng. Aspects* *215*, 221 (2003).
39. Hunger M., Brouwers H.J.H.: *Cement & Concrete Composites* *31*, 39 (2008).
40. Masteau J.C., Thomas G.: *Powder Technology* *101*, 240 (1999).
41. Grady D.E.: *J Appl Phys* *53*, 322 (1981).
42. Grady D.E.: *Int. J. Fract.* *163*, 85 (2010).
43. Qi Ch., Wang M., Qian Q.: *Journal of Impact Engineering* *36*, 1355 (2009).